

# Future evolution of slope stability analysis created by SPH method

## Évolution future de l'analyse de stabilité des pentes créé par la méthode SPH

Nonoyama H.  
Nagoya University, Japan

Yashima A., Moriguchi S.  
Gifu University, Japan

**ABSTRACT:** In this paper, the SPH (Smoothed Particle Hydrodynamics) method is applied to slope stability problems. This method can handle large deformation problems because it is based on the free mesh system. In addition, the constitutive models of geomaterials can be used directly. First, a simulation of a simple shear test is carried out to validate the SPH method. Then, slope stability analysis considering countermeasures is carried out. The numerical results are compared with results of the safety factors calculated by the Fellenius method. Based on the obtained results, the effectiveness of the SPH method for slope stability analysis is discussed.

**RÉSUMÉ :** Dans cet article, la méthode SPH (hydrodynamique des particules lissées) est appliquée à des problèmes de stabilité des pentes. La méthode peut traiter des problèmes de grandes déformations parce qu'elle est basée sur le système de maillage libre. En outre, les modèles de comportement des géomatériaux peuvent être utilisés directement. Dans un premier temps, une simulation d'essai de cisaillement simple a été réalisée afin de valider la méthode SPH. Ensuite, une analyse de stabilité des pentes considérant des contre-mesures a été réalisée. Les résultats numériques ont été comparés avec les résultats des facteurs de sécurité calculés par la méthode Fellenius. Sur la base des résultats obtenus, l'efficacité de la méthode SPH pour l'analyse de la stabilité des pentes a été discutée.

**KEYWORDS:** slope stability analysis, meshfree method, constitutive model

### 1 INTRODUCTION

In terms of the slope stability problems, design of structures and evaluation of countermeasures are carried out using a safety factor of slope obtained from circular slippage calculations at the practical level. In this approach, the safety factor of the slope is easily obtained from equilibrium of force. However, it is not possible to take into account of the deformation of slope. If it is possible to predict the deformation of slope, more detailed design of structures and evaluation of countermeasures can be facilitated. A lot of deformation analyses using the Finite Element Method (FEM) with developed constitutive models have been reported. It is, however, still difficult to solve large deformation problems using the FEM due to the distortion of the mesh. On the other hand, to solve such problems, various numerical approaches have been proposed, such as a modeling based on the computational fluid dynamics (CFD) and the discrete modeling (Cundall and Strack 1979). In the method based on CFD, it is not necessary to pay attention to mesh distortion, because the mesh is fixed in space. However, soils are assumed to be a kind of non-Newtonian fluids (Moriguchi 2005). Thus this modeling is an effective tool for flow problems, but is difficult to apply to static deformation problems. In addition, it is difficult to use constitutive models based on solid mechanics, because they cannot easily handle the history information of soils during deformation. The discrete modeling uses an assembly of discrete elements, and is inappropriate for dealing with constitutive models based on a continuum approximation.

Against these backgrounds, the purpose of this research is to express the large deformation behavior of geomaterials in the framework of continuum mechanics. The smoothed particle hydrodynamics (SPH) method, proposed by Lucy (1977) and Gingold and Monaghan (1977), is based on a mesh-free Lagrangian scheme, and is one of the effective numerical methods. The method can solve large deformation problems

without mesh distortion. Moreover, it can handle the governing equations and existing constitutive models for geomaterials, since it is based on a continuum approximation. The method has already been used to solve many types of geotechnical problems, and a number of interesting achievements have been published (e.g., Maeda et al. 2004, Bui 2007). From these achievements, it is shown that the SPH is applicable to geotechnical problems. However, as far as the introduction of the constitutive models of geomaterial into the SPH method, detailed discussions have not been carried out.

In this paper, the SPH method was applied to slope stability problems. In order to validate the method, a simulation of the simple shear test for elasto-plastic materials is carried out. Then, a slope stability analysis considering countermeasures is carried out. The numerical results are compared with the results of the Fellenius method. Based on the obtained results, the effectiveness of the SPH method for slope stability analysis is discussed.

### 2 NUMERICAL METHOD

#### 2.1 Basic theory of SPH method

In the SPH method, an object is expressed as an assembly of particles. If the motions of the particles are solved individually, the deformation behavior of the continuum cannot be represented by this technique. In order to treat an object as a continuum, a unique interpolation theory is used. This interpolation theory includes two key approximations: a kernel approximation and a particle approximation. The first step is a kernel approximation of the field functions. The kernel approximations are based on neighboring particles  $\beta$  located at points  $x^\beta$  within the support domain  $\kappa^d h$  of a smoothing function  $W$  for a reference particle  $\alpha$  located at point  $x^\alpha$ , as shown in Fig. 1. In the first step of the interpolation, we define a smoothed

physical quantity  $\langle f(x^\alpha) \rangle$  for the physical quantity  $f(x^\alpha)$  at the reference particle  $\alpha$  as follows:

$$\langle f(x^\alpha) \rangle = \int_{\Omega} f(x^\beta) W(r, h) dx^\beta \quad (1)$$

where  $r = |x^\alpha - x^\beta|$ ,  $h$  is the radius of the influence domain, and  $\Omega$  is the volume of the integral that contains  $x^\alpha$  and  $x^\beta$ .

In the second step of the interpolation, the physical quantity  $\langle f(x^\alpha) \rangle$  for the reference particle  $\alpha$  is expressed as the summation of the distribution of the assumed physical quantities  $f(x^\beta)$  for each particle. Thus, the physical quantity can be expressed in terms of  $N$  discrete points:

$$\langle f(x^\alpha) \rangle = \sum_{\beta} \frac{m^\beta}{\rho^\beta} f(x^\beta) W^{\alpha\beta} \quad (2)$$

where  $m^\beta$  is the mass, and  $\rho^\beta$  is the density of neighboring particles  $\beta$ .  $N$  is the numbers of neighboring particles in the support domain, and  $W^{\alpha\beta}$  is the smoothing function that expressed the contribution from the neighboring particles  $\beta$  to the reference particle  $\alpha$ . In this study, Cubic spline function (Swegle 1994) is used as the smoothing function. Equation (2) is a formula for evaluating a physical quantity via the SPH method. It is also possible to approximate the spatial gradient of a physical quantity in a similar way, using the spatial derivative of the smoothing function. The spatial derivative of Eq. (2) can be written as

$$\frac{\partial \langle f(x^\alpha) \rangle}{\partial x_i} = \sum_{\beta} \frac{m^\beta}{\rho^\beta} f(x^\beta) \frac{\partial W^{\alpha\beta}}{\partial x_i} \quad (3)$$

Based on the two-step interpolation procedure, it is possible to calculate any physical quantity and its special derivative of a physical quantity.

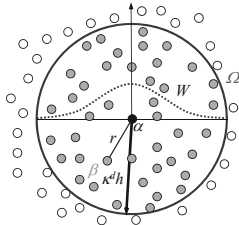


Figure 1. An image of basic concept of SPH method

## 2.2 SPH method based on the solid mechanics

The governing equations used in this study are based on solid mechanics. The equation of continuity and the equation of motion can be defined as follows,

$$\frac{d\rho}{dt} = -\rho \frac{\partial u_i}{\partial x_i} \quad (4)$$

$$\frac{du_i}{dt} = \frac{1}{\rho} \frac{\partial \sigma_{ij}}{\partial x_j} + F_i \quad (5)$$

where  $u_i$  is the velocity vector,  $\rho$  is the density,  $\sigma_{ij}$  is the stress tensor and  $F_i$  is the external force vector. Applying the SPH interpolation theories, the equations are expressed as follows:

$$\frac{d\rho^\alpha}{dt} = -\sum_{\beta} m^\beta (u_i^\beta - u_i^\alpha) \frac{\partial W^{\alpha\beta}}{\partial x_i} \quad (6)$$

$$\frac{du_i^\alpha}{dt} = \sum_{\beta} m^\beta \left( \frac{\sigma_{ij}^\alpha}{(\rho^\alpha)^2} + \frac{\sigma_{ij}^\beta}{(\rho^\beta)^2} + C_{ij}^{\alpha\beta} \right) \frac{\partial W^{\alpha\beta}}{\partial x_j} + F_i^\alpha \quad (7)$$

where  $C_{ij}$  is the summation of the artificial viscosity term (Monaghan and Gingold 1983) and the artificial stress term (Monaghan 2000; Gray et al. 2001). In order to introduce the artificial viscosity and the artificial stress, the numerical instability and the tensile instability are decreased (Swegle et al. 1995). Tensile instability, specifically the instability of the solution for tension deformation, is one of the problems with the SPH method for solid mechanics. In this study, the Drucker-Prager model (Drucker and Prager 1952) and the Super-subloading Yield Surface Modified Cam-clay model (Asaoka et al. 2000; 2002) are used in the deformation analysis of geomaterial to validate potential of the SPH method.

## 3 SIMULATION OF SIMPLE SHEAR TEST

In the validations of the SPH method for solid mechanics, a simulation of simple shear test under plane strain condition is carried out using Drucker-Prager model and Super-subloading Yield Surface Modified Cam-clay model. Calculated stress strain relation and stress paths are compared with the theoretical solution at the center of specimen. Figure 2 illustrates the numerical model used in the simulation. As the figure indicates, the specimen is a square object (10 cm by 10 cm). In the SPH method, numerical instabilities and errors tend to arise due to lack of calculation points. Therefore, a virtual area surrounded the specimen was used in this simulation. The solid line denotes the initial configuration of the specimen, and the dashed line denotes the configuration after deformation. In the simulation, the virtual area is forcibly deformed with a constant displacement to represent simple shear conditions, and the deformation of the specimen is calculated. Since a virtual area surrounded the specimen, only the scheme is employed in this validation. The parameters used in this simulation are summarized in Tables 1. As Table 1 indicates, seven different cases are considered in this simulation. In Cases 1, cohesive frictional material is used. In Cases 2 and 3, parameters of typical clay under two different values of the initial mean stress and initial overconsolidation ratio are used. In Cases 4 to 7, parameters of typical sand under three different values of the initial mean stress and degree of structure are utilized.

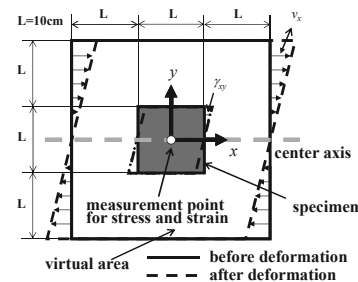


Figure 2. Numerical model

Figures 3 to 5 shows calculated stress-strain relation and stress paths at the center of the specimen. The theoretical solutions are also described in these figures for comparison. The solid line denotes the theoretical solutions, and plotted points indicate the obtained results. Based on the comparison, the results from the SPH scheme are in good agreement with the theoretical solution. Also, by introducing the Super-subloading Yield Surface Modified Cam-clay model (Asaoka et al. 2000; 2002) into the method, the softening with plastic compression behavior of structured soil and rewinding behavior of overconsolidated clay (Fig. 4) are expressed. Also, the softening behaviors with plastic compression of medium-dense sand and subsequent hardening behavior with plastic expansion (Fig. 5)

are expressed. It is summarized that the high performance elasto-plastic constitutive model can be introduced into the SPH method. Also, it is possible to simulate the various state of geomaterial, such as the clay and sand, using the SPH method.

Table 1. Material parameters

(a)Drucker-Prager model

Case		1
Young's modulus	$E$ [kPa]	1000.0
Poisson's ratio	$\nu$	0.33
cohesion	$c$ [kPa]	50.0
internal friction angle	$\phi$ [deg]	30.0
initial mean stress	$p_0$ [kPa]	98.0

(b) Super-subloading Yield Surface Modified Cam-clay model

Case		2	3	4	5	6	7
<b>&lt;elasto-plastic parameters&gt;</b>							
compression index	$\lambda$	0.200		0.052			
swelling index	$\kappa$	0.050		0.010			
critical state constant	$M$	1.40		1.0			
NCL intercept	$N$	2.20		1.98			
Poisson's ratio	$\nu$	0.3					
<b>&lt;evolution parameters&gt;</b>							
degradation index of overconsolidation	$m$	3.0		0.06			
degradation index of structure	$a$	0.5		2.2			
degradation index of structure	$b=c$	1.0					
<b>&lt;initial value&gt;</b>							
initial degree of overconsolidation	$1/R_0$	5.01	1.16	20.0			
initial degree of structure	$1/R_0^*$	5.0	1.40	10.0	23.6	39.0	
initial specific volume	$v_0$	2.20		1.95			
initial mean stress	$p_0$ [kPa]	98.1	294.3	20.0	98.1	196.2	294.3

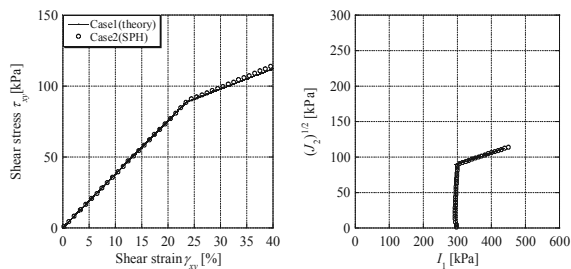


Figure 3. Drucker-Prager model (Case 1)

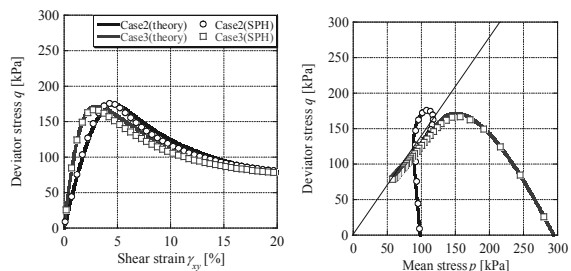


Figure 4. Super-subloading Yield Surface Modified Cam-clay model (Cases 2 and 3)

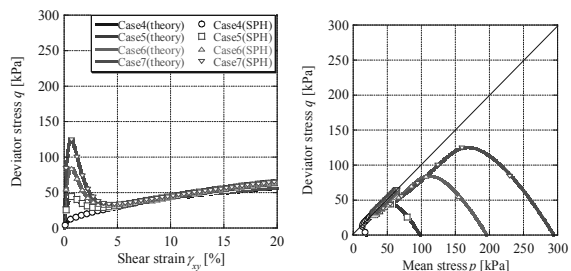


Figure 5. Super-subloading Yield Surface Modified Cam-clay model (Cases 4 to 7)

4 SLOPE STABILITY ANALYSIS CONSIDERING COUNTERMEASURES

A slope stability analysis considering countermeasures is carried out, using the Drucker-Prager model. Two types of countermeasures, such as top soil removal work and counterweight fill, are considered into these simulations. The numerical results are compared with results obtained using the safety factors calculated by the Fellenius method. Figure 6 illustrates the numerical models in Cases 1 to 8. The slope angle is 45 degrees and the model ground is cohesive. Also, as the figure shows, the displacements at the top of the slope are checked. The parameters used in this simulation are listed in Table 2. For the boundary conditions, the horizontal direction at the side wall of the slope was fixed, and the vertical direction is free. The horizontal and vertical directions at the bottom of the embankment are fixed. Fixed boundary particles are used to describe the walls. In order to take into account the effect of surface compaction, the internal friction angle of the counterweight fill material is set to 30 degrees. The effect of pore water pressure is not taken into account. The isotropic stress corresponding to static earth pressure is used as the initial stress.

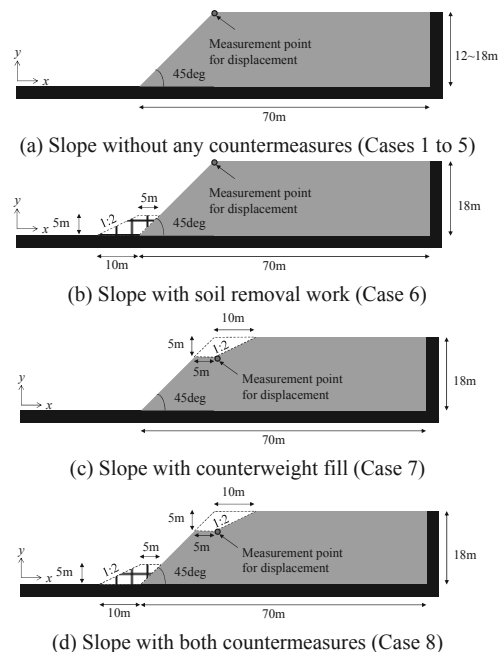


Figure 6. Numerical models.

Table 2. Material parameters.

Young's modulus	$E$ [MPa]	100.0
Poisson's ratio	$\nu$	0.30
cohesion	$c$ [kPa]	50
internal friction angle	$\phi$ [deg]	30
unit weight	$\gamma$ [kN/m <sup>3</sup> ]	19.6

Table 3. Safety factors obtained from the Fellenius method for each case.

Case	Countermeasures	Height of slope $H$ [m]	safety factor $F_s$
1	Without any countermeasures	12	1.24
2		14	1.01
3		15	0.91
4		16	0.86
5	Soil removal work	18	0.75
6			0.87
7			0.90
8			1.02

The safety factors obtained from the Fellenius method are listed in Table 3. As Table 3 indicates, the safety factors rise according to the order of case without any countermeasures,

case with soil removal work, case with counterweight fill, and case with both soil removal work and counterweight fill.

The distributions of accumulation of the maximum shear strain are shown in Fig. 7. As explained in above, boundary particles are used for the wall, but are not shown in these figures. Figure 8 shows the relationship between the safety factor and the value obtained by dividing the displacement  $\delta$  at the top of the slope by the height of the slope  $H$ . When the safety factor is larger than 1.0 (Cases 1 and 2), shear strain does not appear in the figures. However, when the safety factor is less than 1.0 (Cases 3 to 5), a distribution of circular shear strain can be seen. When the safety factor is close to 0.9, shear strain is observed but still large deformation cannot be observed. In particular, a crack forms at the crown of the slope, and block slippage is confirmed in the cases with the lowest safety factors. In the case without any countermeasures (Case 5), the shear strain is conspicuous and the slope is largely deformed. On the other hand, in the cases with countermeasures (Cases 6 to 8), the shear strain does not become more prominent and the displacements can be controlled as the safety factor increased. Thus, similar tendencies are observed in the results from the SPH method and the Fellenius method. In addition, while conventional circular slippage calculations are used to estimate the occurrence of rigid block slippage, the SPH method can estimate not only the stability, but also the effects of deformation. In Cases 3 and 7, the slope is not deformed, although the safety factor is less than 1.0. On the boundary between stable and unstable states, we consider that the slope is stabilized due to the redistribution of stress following an initial small deformation. The SPH method can estimate deformation and stability simultaneously. Moreover, it is capable of continuously predicting the deformation, even in a large deformation region. In other words, the SPH method can predict the entire deformation process of a geomaterial. Therefore, one may conclude that a variety of useful information about slope stability problems can be obtained via the SPH method.

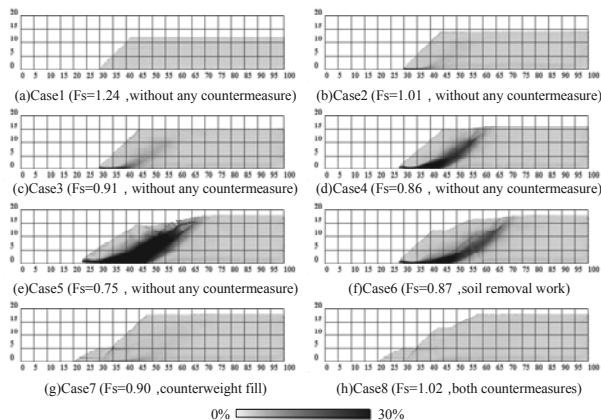


Figure 7. Distributions of accumulation of the maximum shear strain

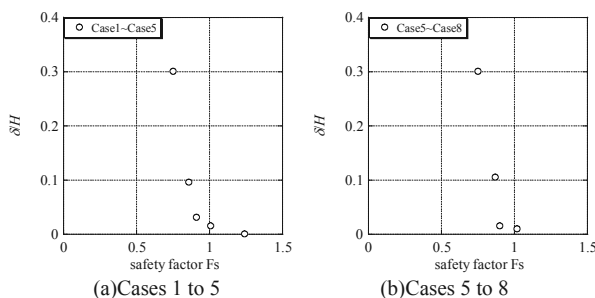


Figure 8. Relationship between safety factor and displacement at the top of slope.

## 5 CONCLUSION

In this study, introducing the constitutive model into the SPH method, deformation analyses of geomaterials were carried out. Firstly, in order to validate the method, the simulation of simple shear test of elasto-plastic material was simulated using two kinds of constitutive models of geomaterials. The numerical results were compared with the theoretical solutions. Then, a slope stability analysis considering countermeasures was carried out. The conclusions can be summarized as follows:

- The simulation of a simple shear test demonstrated that the SPH method could calculate the appropriate stress state of geomaterials using high performance elasto-plastic constitutive models.
- The SPH method was applied to slope stability analysis. The results indicated that the method was able to express the same safety factor tendencies obtained from the conventional circular slippage calculations. At the same time, the SPH method can simultaneously estimate both the deformation and stability. From the results of a slope stability analysis considering countermeasures, it can be inferred that the SPH method was capable of predicting the deformation and stability of slopes even in complex situations, such as simulations that include countermeasures.
- From a series of the numerical results, the SPH method was found to be applicable to slope stability analysis. Also, the SPH method has the potential to describe the deformation of geomaterials from the initial state to subsequent large deformations.

## 6 REFERENCES

- Asaoka A. et al. 2000. Superloading yield surface concept for highly structured soil behavior, *Soils and Foundations*, 40 (2), 99-110.
- Asaoka A. et al. 2002. An elasto-plastic description of two distinct volume change mechanisms of soils, *Soils and Foundations*, 42 (5), 47-57.
- Bui, H.H. 2007. Lagrangian mesh-free particle method (SPH) for large deformation and post-failure of geomaterial using elasto-plastic constitutive models, *Ph.D. Dissertation of Ritsumeikan University, Japan*.
- Cudall P.A. and Strack O.D.L. 1979. A discrete numerical model for granular assemblies, *Geotechnique*, 29 (1), 47-65.
- Drucker D.C. and Prager W. 1952. Soil mechanics and plastic analysis for limit design, *Quart. Appl. Math.*, 10 (2), 157-165.
- Gingold R.A. and Monaghan J.J. 1977. Smoothed particle hydrodynamics: theory and application to non-spherical stars, *Monthly Notices Roy. Astron. Soc.*, 181, 375-389.
- Gray J.P. et al. 2001. SPH elastic dynamics, *Comput. Methods Appl. Mech. Engrg.*, 190, 6641-6662.
- Lucy L.B. 1977. A numerical approach to the testing of the fission hypothesis, *Astron. J.*, 82, 1023-1024.
- Maeda K. and Sakai M. 2004. Development of seepage failure analysis procedure of granular ground with Smoothed Particle Hydrodynamics (SPH) method, *J. Appl. Mech.*, JSCE, 7, 775-786 (in Japanese).
- Monaghan J.J. and Gingold R.A. 1983. Shock simulation by the particle method SPH, *J. Comput. Phys.*, 52, 374-389.
- Monaghan J.J. 2000. SPH without a tensile instability, *J. Comput. Phys.*, 159, 290-311.
- Moriguchi S. 2005. CIP-based numerical analysis for large deformation of geomaterials, *Ph.D. Dissertation of Gifu University, Japan*.
- Sweple J.W. et al. 1994. An analysis of smoothed particle hydrodynamics, *SAND93-2513, Sandia National Laboratories, Albuquerque, NM*.
- Sweple J.W. et al. 1995. Smoothed particle hydrodynamics stability analysis, *J. Comput. Phys.*, 116(1), 123-134.